Biorheology 41 (2004) 577–590
IOS Press

Functional tissue engineering of chondral and osteochondral constructs

Eric G. Lima [a], Robert L. Mauck [a,*], Shelley H. Han [a], Seonghun Park [b], Kenneth W. Ng [a], Gerard A. Ateshian [a,b] and Clark T. Hung [a,**]

[a] *Department of Biomedical Engineering, Columbia University, New York, NY, USA*
[b] *Department of Mechanical Engineering, Columbia University, New York, NY, USA*

Abstract. Due to the prevalence of osteoarthritis (OA) and damage to articular cartilage, coupled with the poor intrinsic healing capacity of this avascular connective tissue, there is a great demand for an articular cartilage substitute. As the bearing material of diarthrodial joints, articular cartilage has remarkable functional properties that have been difficult to reproduce in tissue-engineered constructs. We have previously demonstrated that by using a functional tissue engineering approach that incorporates mechanical loading into the long-term culture environment, one can enhance the development of mechanical properties in chondrocyte-seeded agarose constructs. As these gel constructs begin to achieve material properties similar to that of the native tissue, however, new challenges arise, including integration of the construct with the underlying native bone. To address this issue, we have developed a technique for producing gel constructs integrated into an underlying bony substrate. These osteochondral constructs develop cartilage-like extracellular matrix and material properties over time in free swelling culture. In this study, as a preliminary to loading such osteochondral constructs, finite element modeling (FEM) was used to predict the spatial and temporal stress, strain, and fluid flow fields within constructs subjected to dynamic deformational loading. The results of these models suggest that while chondral ("gel alone") constructs see a largely homogenous field of mechanical signals, osteochondral ("gel bone") constructs see a largely inhomogeneous distribution of mechanical signals. Such inhomogeneity in the mechanical environment may aid in the development of inhomogeneity in the engineered osteochondral constructs. Together with experimental observations, we anticipate that such modeling efforts will provide direction for our efforts aimed at the optimization of applied physical forces for the functional tissue engineering of an osteochondral articular cartilage substitute.

Keywords: Functional tissue engineering, deformational loading, articular cartilage, osteochondral constructs, finite element models

1. Introduction

Damage to articular cartilage is a common condition affecting the joints of millions of people in the U.S. alone. This damage is complicated by the poor regenerative capacity of adult articular cartilage and the disability and pain that accompanies these injuries [30]. Nearly 10% of the U.S. population aged 30 and older has clinical osteoarthritis (OA) of the hip or knee, with total direct costs estimated at $28.6 billion dollars per year [15]. There exists a range of clinical options (short of total joint replacement) with variable degrees of success, for the repair of focal lesions and damage to the articular surface. These

*Present address: Cartilage Biology and Orthopaedics Branch, National Institute of Arthritis, Musculoskeletal & Skin Diseases, NIH, Bethesda, MD, USA.
**Address for correspondence: Clark T. Hung, PhD, Columbia University, Department of Biomedical Engineering, 351 Engineering Terrace, MC8904, 1210 Amsterdam Avenue, New York, NY 10027, USA. Tel.: +1 212 854 6542; Fax: +1 212 854 8725; E-mail: cth6@columbia.edu.

approaches include tissue adhesives (e.g., [3,21]), enzymatic treatments [13], laser solder welding [61], autograft cell/tissue transfer via periosteal grafts [41], autologous osteochondral grafting such as mosaicplasty [20] and the Carticel method [8]. While promising in many respects, these approaches are limited by the amount of tissue available for such procedures, as well as donor site morbidity associated with its harvest. The poor intrinsic healing capacity along with the lack of effective clinical repair strategies has generated great interest in the engineering of replacement cartilage tissues.

The most prevalent approach to cartilage tissue engineering involves the combination of chondrocytes (or mesenchymal progenitor cells) with scaffolds (fibrous meshes or hydrogels) for long-term culture. Such constructs have been grown both statically (i.e., in Petri dishes or in the backs of nude mice) and in sophisticated bioreactors designed to provide a nutrient rich environment for construct development [2,14,16,17,43,45,51,52]. In our studies, the underlying premise has been that the application of physiologic deformational loading, as part of the culture environment, will promote development of cartilage tissue engineered constructs having functional load-bearing tissue properties. The rationale for such an approach is based on the well-characterized response of chondrocytes to a variety of physical stimuli that arise with loading of diarthrodial joints (see review in [18]). More specifically, we have used the application of uni-axial unconfined dynamic deformational loading (1 Hz, 10% peak-to-peak deformation) of chondrocyte-seeded agarose constructs to encourage tissue growth *in vitro*. This mode of deformational loading was chosen as it engenders mechanical signals in gels similar to that seen in the native tissue with joint contact (Fig. 1, [44]). To carry out such studies, we employed agarose hydrogels, which not only provide a 3D environment that maintains the chondrocyte phenotype and allows for the development of a functional extracellular matrix [7,9,10], but also can withstand deformational loading from the outset of encapsulation, without any significant pre-incubation period. With time in culture, chondrocyte-seeded agarose hydrogels increase in tissue properties and respond to short-term applied deformational loading in a manner similar to native tissue [11,26,27]. Furthermore, long-term deformational loading of these constructs increases the rate and extent of development of tissue properties compared to free swelling controls [31–35]. As these engineered constructs approach the mechanical and biochemical properties of the native tissue, significant new challenges become apparent [4,42]. In particular, integration of these constructs into the damaged articular surface remains a difficult problem [4,42,60].

One possible solution to the problem of integration may be the development of engineered osteochondral constructs [5,24,46–48] similar to those used for autologous transplantation [1,20]. A number of different approaches have explored the generation of such constructs, employing a diverse spectrum of scaffolds and cell populations [5,24,46–48]. In a previous study, we suggested the production of osteochondral constructs composed of a cell-seeded agarose layer integrated with a trabecular subchondral bony layer, with the hypothesis that the bone layer would provide a suitable interface for *in vivo* bony ingrowth [24]. Osteochondral constructs of this composition (seeded with primary bovine chondrocytes) were shown to increase in biochemical and mechanical properties with time in free swelling culture [24], indicating that the culture method is conducive to cartilage-specific tissue growth.

Dynamic deformational loading has been shown to improve the mechanical properties of chondrocyte-seeded agarose constructs. This approach may similarly prove useful for the culture of osteochondral constructs. A number of interesting issues arise, however, from the intrinsic differences in the stiffness of each layer in such a bilayered construct. First, the trabecular bone region of such constructs is expected to be much stiffer than the region comprised totally of agarose. Consequently one would expect all deformation to occur solely in the agarose gel region. Secondly, the gel is at least partially

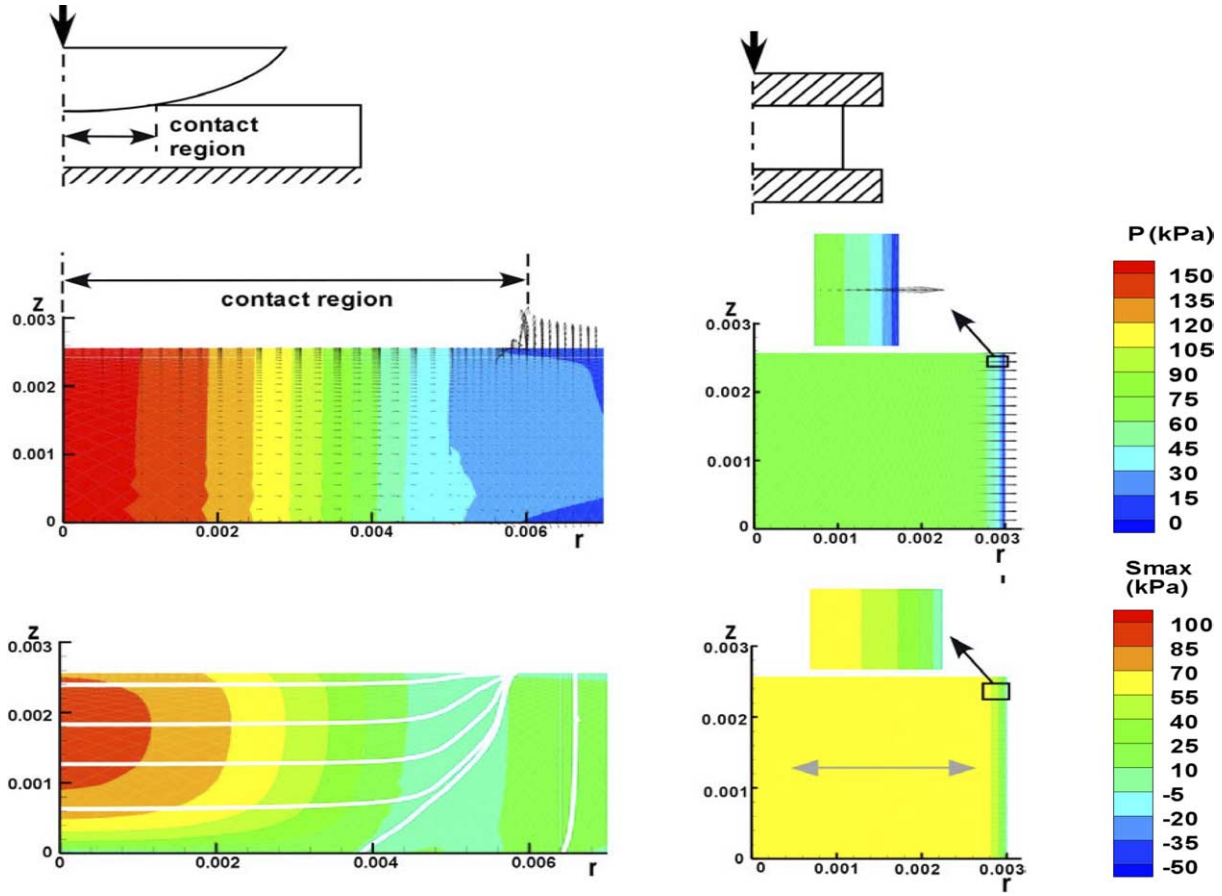

Fig. 1. Finite element prediction of fluid pressure and fluid flow (top) and maximum stress (bottom) occurring within an isotropic articular cartilage layer loaded in contact (left) and a cartilage disk loaded in unconfined compression. Note the similarity between the two loading conditions in mechanical signals generated near the point of contact. Adapted from [44].

infused into the bone along the gel bone interface. Such fixation would be expected to restrict the lateral expansion of the gel layer with axial deformation, and control the movement of fluid through these regions of differing permeability. Given these differences in boundary conditions brought about by the inclusion of a bony layer, the goals of the current study were three-fold. First, we were interested in examining the bulk mechanical properties of acellular agarose constructs with and without a bony layer to determine if inclusion of a bony layer would alter the overall mechanical behavior. Second, we tested the hypothesis that deformation would occur solely within the gel layer of osteochondral constructs. Third, we used biphasic finite element models to compare the differing mechanical stimuli that are predicted to arise with dynamic deformational loading of osteochondral constructs compared to those that occur in gel alone constructs in response to the same mechanical loading protocol. To gain an appreciation of the implication of these spatially-ranging mechanical stimuli on cell activities, gene expression was performed on dynamically-loaded chondral (gel-alone) and osteochondral (gel-bone) constructs.

2. Materials and methods

2.1. Osteochondral construct preparation

Cylindrical trabecular bone cores, ∅5 mm × 4 mm thick, were harvested from the epiphysis of metatarsal bones of 3 month-old calves (Fig. 2). Cores were cut to size with a diamond saw, cleaned of marrow with a water pick, and mass and volume measurements were taken to determine the apparent density. Cores were grouped by density, and infused with a molten 3% (in PBS) agarose hydrogel (Type VII, Sigma) in a custom mold to produce constructs with an ∼2 mm gel-only region, an ∼2 mm gel-bone interface region, and a ∼2 mm bone-only region, as described previously [24].

2.2. Bulk mechanical testing

Five constructs per group were tested in unconfined compression as in [35], with stress relaxation tests to 10% strain (of upper gel thickness) followed by dynamic testing (with an applied displacement of 20 μm) at frequencies ranging from 0.005–1 Hz. The Young's modulus was determined from the equilibrium reaction force (taken at >1200 seconds) and the specimen geometry, while the dynamic modulus was calculated from the maximum peak-to-peak stress normalized to the maximum peak-to-peak strain.

2.3. Displacement fields

To obtain an axial displacement field, osteochondral constructs were cut in half and compressed using a custom compression device mounted on the stage of an inverted microscope, as described in [53]. The initial thickness of the specimen was measured optically (1.66 μm/pixel) and a 5% tare strain (of the gel thickness) was applied. After equilibrium, an image was acquired, and the specimen was further compressed another 5% strain increment with a second image acquired after equilibrium. Image analysis was performed using an automated digital image correlation technique to produce an axial displacement field [53,54,57].

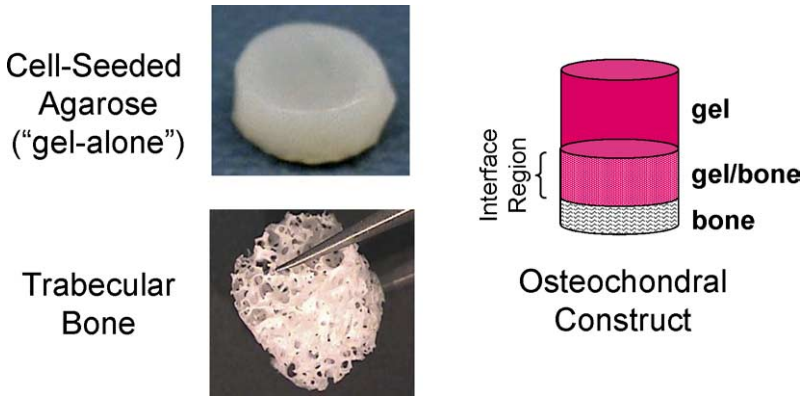

Fig. 2. Schematic for making bilayered osteochondral constructs composed of a gel layer (agarose) interpenetrated into a subchondral bony substrate. Constructs can be formed with a defined geometry and gel penetration depth.

2.4. Biphasic finite element models

Finite element meshes were defined with a commercial software package (I-DEAS, SDRC, Plano, TX) to model gel-alone agarose constructs (2 mm thickness $\times$ 5 mm diameter) and osteochondral composite constructs (4 mm thickness $\times$ 5 mm diameter), with a variable gel bone interface region (0–100% of bone layer thickness), Fig. 5. Meshes were defined as axisymmetric, and contained 600 elements per mesh with eight nodes per element, with the distribution of elements biased towards the free edge of the construct. Each region was assumed homogenous, with a linear isotropic elastic solid matrix, with the agarose gel region having $E_Y = 10$ kPa, $\nu = 0.3$, $k = 1 \times 10^{-12}$ m^4/N s, the gel-bone region having $E_Y = 1000$ MPa, $\nu = 0.3$, $k = 0.25 \times 10^{-12}$ m^4/N s, and the bone region having $E_Y = 1000$ MPa, $\nu = 0.3$, $k = 1 \times 10^{-8}$ m^4/N s. The degree gel penetration was set at 0, 25, 50, 75, and 100% of the underlying bony thickness. A custom FEM program (as described in [44]) incorporating biphasic theory [38] was used to solve the problem of unconfined deformational loading of such constructs in both stress relaxation (to 10% gel thickness deformation) and with an applied sinusoidal deformation of 10% of the gel thickness at a frequency of 1 Hz. The resulting fluctuations in mechanical signals generated within each construct were output and analyzed at equilibrium for stress relaxation testing ($t = 1000$ s) or at the point of maximal compressive axial deformation ($t = 0.5$ s) for the case of dynamic deformational loading.

2.5. Gene expression

Gene expression was analyzed for previously frozen chondrocyte-seeded (60×10^6 cells/ml) chondral and osteochondral constructs that had been dynamically loaded for 6 hours to 10% of the gel thickness as in [35]. The gel and bone regions of the osteochondral constructs were carefully separated under RNase free conditions using a scalpel. Two samples were pooled and homogenized using a mortar and pestle for the disc and gel region and a mechanical homogenizer for the bone region. RNA was isolated from the samples by two successive guanidine hydrochloride extractions [22] followed by a TRIzol® (Invitrogen, Life Technologies) extraction. Total RNA concentration was measured using a spectrophotometer at a 260 nm wavelength (μQuant, Bio-Tek Instruments). A reverse transcription polymerase chain reaction (RT-PCR) was carried out using the SuperScript™ First-Strand Synthesis System for RT-PCR (Invitrogen, Life Technologies) to determine relative mRNA expression levels for aggrecan and Type II Collagen using glyceraldehyde phosphate dehydrogenase (GAPDH) as an internal control. 500 ng of total RNA in a 20 μl volume was used for the reverse transcription reaction. One microliter of cDNA was used for each PCR reaction using primer sets for Type II Collagen, aggrecan, and GAPDH. Primer sequences were aggrecan (sense): CACTGTTACCGCCACTTCCC, (antisense): GACATCGTTCCACTCGCCCT; Type II Collagen (sense): ATGACAATCTGGCTCCCAAC, (antisense): GCCCTATGTCCACACCGATT; GAPDH (sense): GGTGATGCTGGTGCTGAGTA, (antisense) ATCCACAGTCTTCTGGGTGG. Thirty cycles of PCR were carried out using annealing temperatures of 51°C, 61°C, and 58°C respectively. PCR products were separated on 2% agarose gels containing ethidium bromide, and the bands were digitized and quantified (ImageJ, NIH). Aggrecan and Type II Collagen mRNA levels were normalized by GAPDH for each sample ($n = 6$–8 per group). Data was analyzed by first normalizing the gene expression of dynamically-loaded constructs by the average expression of the corresponding free-swelling control. Three groups were studied: gel-alone (chondral), bone region (lower portion of osteochondral constructs) and gel region (upper portion of osteochondral constructs). One-way analysis of variance with Fisher's LSD test was used to detect significant difference ($\alpha = 0.05$) among the groups using Statistica software (SYSTAT, IL).

3. Results

Bone cores were found to vary in apparent density, and were grouped into high (0.46 ± 0.05), medium (0.36 ± 0.03), and low (0.24 ± 0.03) density groups. Mechanical testing of acellular agarose osteochondral constructs revealed no statistical difference in the Young's modulus with decreasing density of the underlying trabecular bone compared to gel-alone constructs (Fig. 3). However, the dynamic modulus decreased significantly ($p < 0.05$) in the case of the lowest density subchondral bone osteochondral constructs compared to gel-alone constructs (Fig. 3).

Microscopic evaluation of the axial displacement field of osteochondral constructs in unconfined compression (Fig. 4A) revealed that deformation occurred solely in the gel region (Fig. 4B). A FEM simulation of stress relaxation generated a similar deformation profile at equilibrium (Fig. 4C).

Finite element meshes were constructed to model dynamic deformation of both uniform gel alone constructs and osteochondral constructs with mixed material properties (Fig. 5). The application of dynamic compression to the axial boundaries of these constructs showed quantitative and qualitative differences in the resulting magnitude and distribution of mechanical signals. In particular, radial strain in gel-alone constructs was largely homogeneous, while radial strains were larger in magnitude and heterogeneously distributed in osteochondral constructs (Fig. 6), with the highest strain magnitude observed at the surface of the constructs. Fluid pressurization was observed to be largely uniform through the thickness and radial direction in gel-alone constructs (Fig. 7, top left), while there was a higher, and much less uniform distribution of pressure in osteochondral constructs (Fig. 7, top right, bottom left and right). Fluid flux was directed radially and was greatest at the edges of gel-alone constructs (Fig. 7, top left). In osteochondral constructs, high fluid flows were observed at the radial edge (highest at the interface of the gel layer with the subchondral bone), with some flow through the bottom of the gel into the bone-gel region (Fig. 7, top right, bottom left and right). Significant variation of fluid pressurization occurred in

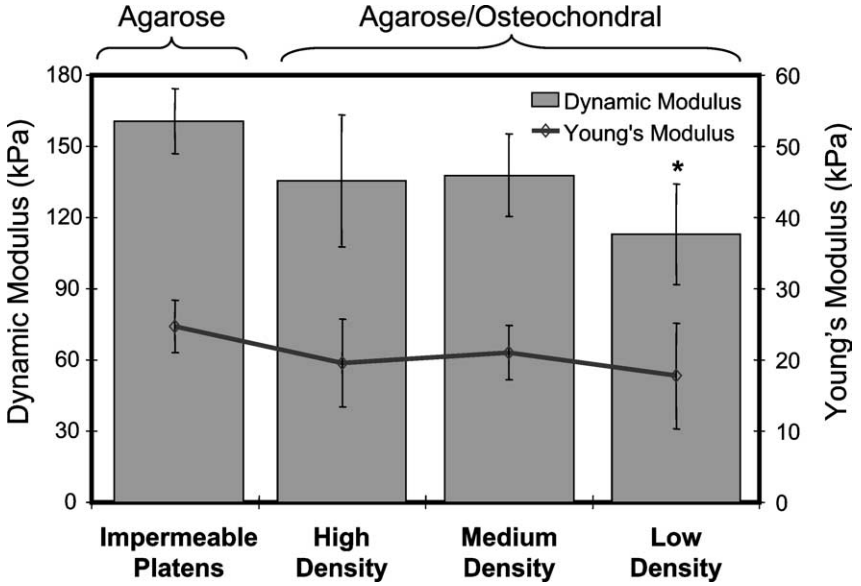

Fig. 3. Dynamic modulus (at 0.5 Hz) and Young's modulus of acellular osteochondral constructs with varying density trabecular bone substrates. * Indicates significant decrease in dynamic modulus compared to gel-alone construct impermeable platen ($p < 0.05$, $n = 5$).

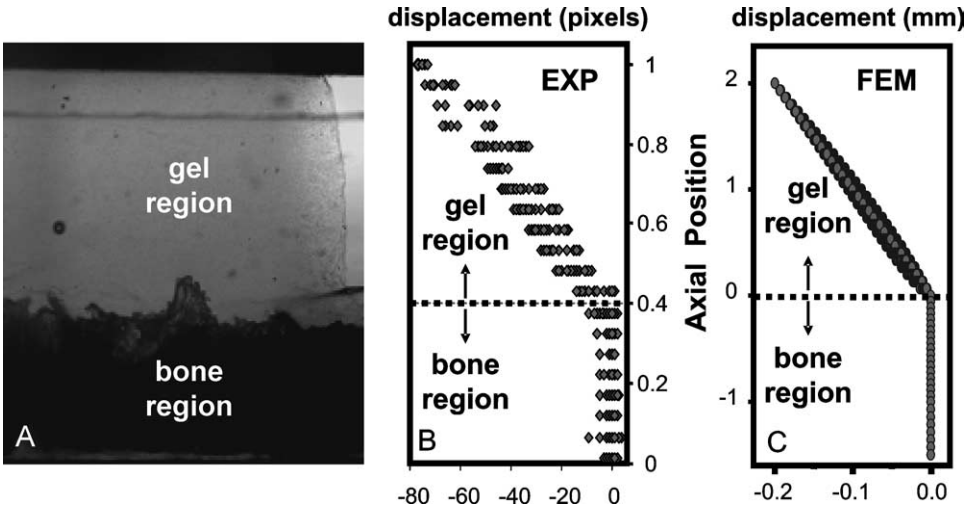

Fig. 4. (A) Cross sectional image of cell-free agarose mounted in a custom microscopy device for measuring local deformation in cartilage and tissue-engineered constructs [53,57]. (B) Measured axial deformation (in pixels) in cell-free osteochondral construct in response to a static axial deformation of 5% of the gel layer thickness. (C) Predicted axial deformation under the same loading conditions (at equilibrium) using the FEM model formulation. Due to the much stiffer bone region, axial deformation occurs solely in the upper gel region.

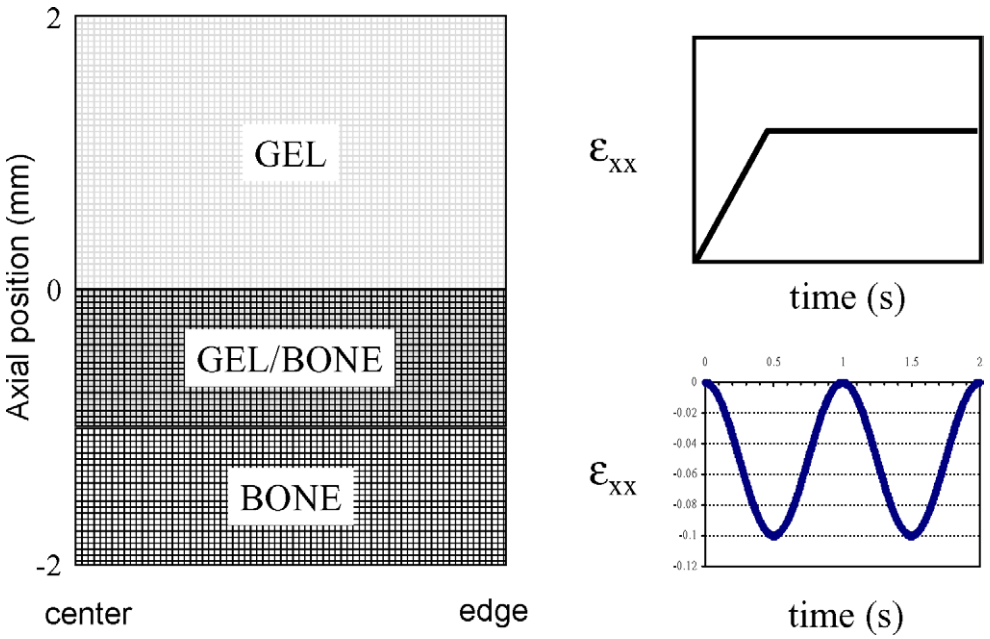

Fig. 5. Finite Element Model (FEM) of osteochondral construct and dynamic loading regime used for analysis.

the bone–gel region as well, and was highest at the gel/bone-gel interface, and decreased to ambient levels at the bone-gel/bone interface. As the penetration of gel into the bony substrate increased form 0% (top right) to 50% (bottom left) to 100% (bottom right) a progressively smaller proportion of fluid flowed through the gel/gel-bone interface, though the distribution of pressure and flow in the superior (chondral) gel region was largely unaffected.

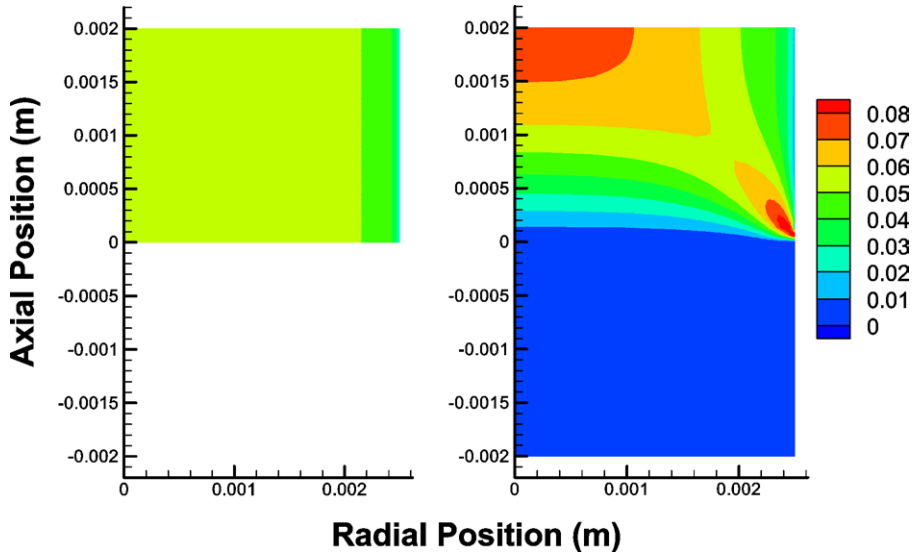

Fig. 6. Radial strain at the peak axial compression of a dynamically loaded (1 Hz, 10% deformation of gel layer thickness) gel alone (left) or gel/bone osteochondral construct (right) as predicted by the biphasic FEM model.

In studies monitoring gene expression of extracellular matrix proteins, the aggrecan and Type II Collagen mRNA levels of chondrocytes in the underlying bone region of osteochondral constructs was significantly elevated compared to that of levels in the upper gel regions ($p < 0.05$, $n = 6$–8), Fig. 8. Additionally, the relative gene expression of chondrocytes in the gel region of these gel-bone constructs was similar to those of chondrocytes residing in gel only constructs.

4. Discussion

Constitutive models coupled with finite element techniques are a useful tool for analyzing complex events occurring in structures that have non-uniform shapes and/or compositions. This preliminary study used biphasic finite element models to compare the predicted mechanical signals that arise in chondral and osteochondral constructs subjected to the same dynamic deformational loading regime. To construct these models, gel constructs were assumed homogenous and isotropic, while osteochondral constructs were given three distinct material regions. The top region of the osteochondral construct, the gel layer, was given the material properties of 2% agarose. Previous work has shown that biphasic theory can adequately predict the mechanical response of agarose hydrogels, particularly during the transient phase of loading [33], and to an even greater extent when one uses a strain-dependent permeability (unpublished observations). The middle region of the osteochondral construct was assigned the permeability of agarose (normalized by the decrease in area brought about by the presence of impermeable bone) and the stiffness of trabecular bone. Finally, the bottom bony region was given the material properties and permeability (very high) of free-draining, cleaned trabecular bone. Such osteochondral constructs, composed of three distinct, but adhered layers, would be expected to alter the mechanical signals generated with deformational loading due to the differing boundary conditions, especially at the gel-gel/bone interface. Similar analyses can be performed for alternate underlying substrate materials (e.g., natural coralline [19], bioactive scaffolds [29], hydrogels [40] and polymers [47]).

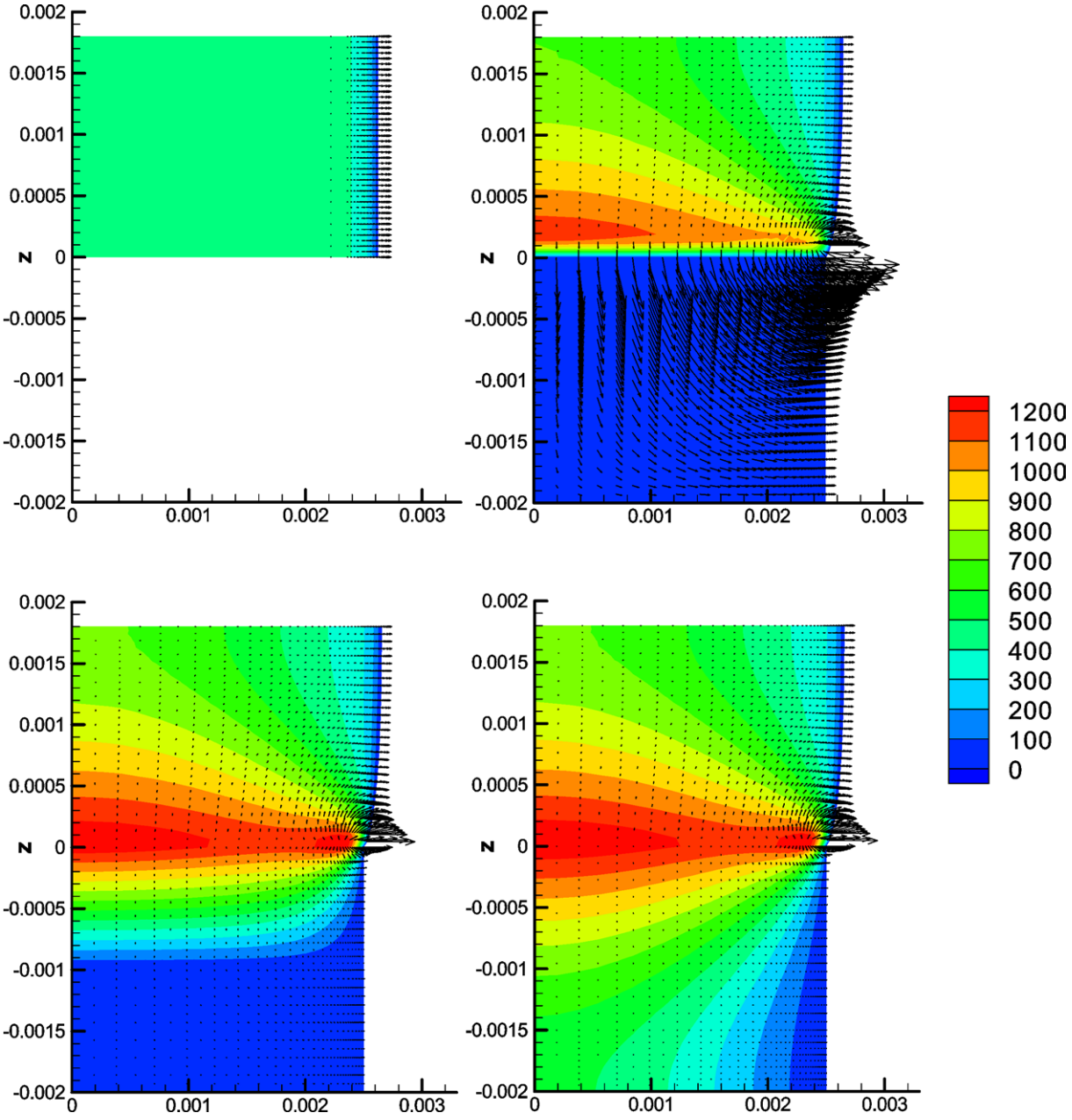

Fig. 7. Hydrostatic pressure (color mapping) and fluid flow (arrows) at the peak axial compression of a dynamically loaded (1 Hz, 10% deformation of gel layer thickness) gel alone (top left) or gel/bone osteochondral construct (top right, bottom left and right) as predicted by the biphasic FEM model.

The results of this study do indeed suggest that the two differing constructs will see disparate mechanical signals through their axial depth and radial position. Experimentally, we first observed that static deformation of an osteochondral construct resulted in deformation occurring solely in the gel region, as one would expect of a construct composed of two layers with such dissimilar material properties. This

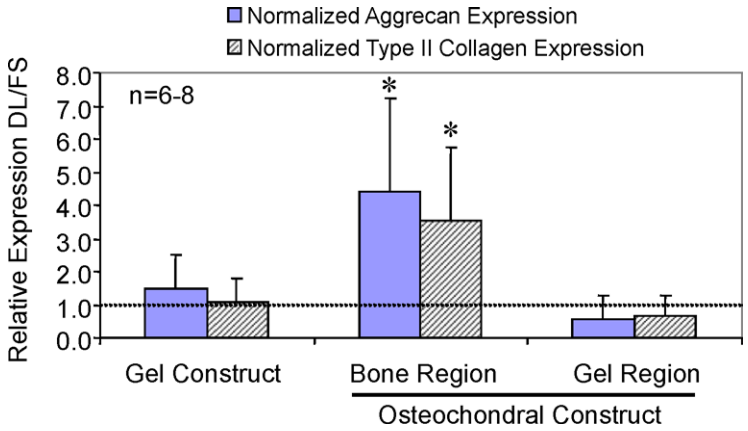

Fig. 8. Relative aggrecan and Type II Collagen gene expression of chondrocyte-seeded gel alone and osteochondral constructs subjected to 6 hours of dynamic loading (1 Hz, 10% deformation). For analysis, osteochondral constructs have been divided into the lower bone region and upper gel regions. Data is normalized to respective free-swelling control constructs and regions. ($^{*}p < 0.05$ versus gel construct and gel region).

deformation profile was linear, as has previously been seen for freshly cast hydrogel constructs, validating our assumption of homogenous material properties in the gel region [56,57]. Using the Biphasic FEM model we were able to predict the form of this deformation by applying the same static deformation to the model and examining the equilibrium response.

While the construct stiffness measured at equilibrium exhibits no relationship with the underlying bone porosity, experimental findings demonstrate that the construct dynamic modulus (a functional measure of the tissue properties that reflects both the matrix stiffness and hydraulic permeability) exhibits a trend of decreasing magnitude with increasing porosity. The latter likely reflects the degree of interstitial fluid pressurization that accompanies dynamic material testing of constructs, which is maximum when the gel is loaded between two impermeable surfaces (permitting only radial fluid exudation during loading) [44]. Since the material properties at equilibrium reflect only the stiffness of the solid construct (when fluid pressurization has subsided) [33], the similar Young's modulus observed over the bone porosity range seems reasonable. These measured bulk (or average) material properties indicate that the presence of an underlying bony substrate can alter the physical environment within the constructs.

FEM analyses can be performed to appreciate the spatial distribution of physical stimuli within the constructs. Using the same FEM model described above, but altering the loading pattern to apply dynamic loading at 1 Hz with a deformation magnitude 10% that of the gel layer thickness of osteochondral (or chondral) constructs reveals more interesting results. In chondral constructs, fluid pressurization and radial strain are similar through the depth and radial position, with only the expected edge effects (both signals rapidly go to zero) [25,36,39]. Fluid flow is also as expected highest at the radial periphery [12]. Dynamic deformational loading of osteochondral constructs, on the other hand, creates hydrostatic pressures, fluid flows, and radial strains that are quantitatively and qualitatively different from those occurring in gel-alone constructs. In particular, at the peak of compression, the gel region of the osteochondral construct experiences significant inhomogeneity in its hydrostatic pressure, with the highest values occurring at the middle of the construct just above the bone interface. Furthermore, radial normal strain is highest at the surface and minimal at the gel/bone interface (where by adhesion

of the two layers the bone keeps the gel from expanding laterally). Finally, as mentioned in the results, osteochondral constructs see the highest levels of fluid flow directed out of the radial edge of the gel region, with a decreasing amount of fluid driven into the bone gel region as the penetration thickness increases.

These findings highlight the differences in mechanical environment that would be seen by cells seeded in the various regions of a dynamically loaded osteochondral construct compared to a gel-alone control. In support of this notion, chondrocyte aggrecan and Type II Collagen gene expression were found to be significantly elevated in the lower bone regions compared to upper gel regions. This finding may suggest that differing regional load-induced signals will likely alter the developing mechanical properties and matrix distribution in osteochondral constructs compared to gel-alone controls [9], and may be harnessed to modulate the development of tissue inhomogeneity in engineered constructs [55,58]. In articular cartilage, tensile stiffness is highest in the most superficial articular cartilage layers [58], and the tension compression non-linearity that derives from this fact is believed to play a role in the frictional response and load bearing capacities of the tissue [6,23,37,49]. In this study, the fact that the highest radial strain with dynamic loading is predicted to occur at the articular surface of the osteochondral construct suggests that such constructs may develop enhanced tensile stiffness in this region (to counteract the strain), and therefore may more closely match important features of the native tissue. Experimental work using cartilage and agarose gels have also shown that cells have maximum biosynthetic activity in regions of high fluid flows [9,12,18,25]. In this study, the prediction of fluid flows through the gel/bone interface may be taken advantage of to encourage subchondral plate formation at the gel–bone interface, and to possibly enhance gel layer-to-bone layer integration strength. The incorporation of pre-seeded bone cells on the underlying substrate may also facilitate development of a subchondral plate [50,59]. Current studies are exploring these possibilities by examining the development of both bulk and local mechanical properties of chondrocyte-seeded agarose bone osteochondral constructs subjected to long-term daily dynamic deformational loading [28].

Acknowledgements

This study was supported by the NIH [R01 AR46568 (CTH), R01 AR46532 (GAA)] and a pre-doctoral fellowship from the Whitaker Foundation (RLM).

References

[1] C.S. Ahmad, Z.A. Cohen, W.N. Levine, G.A. Ateshian and V.C. Mow, Biomechanical and topographic considerations for autologous osteochondral grafting in the knee, *Am. J. Sports Med.* **29**(2) (2001), 201–6.
[2] T. Ahsan, L. Chin, V.W. Wong, A.C. Chen, R.L. Sah, R.A. Bank, N. Verzijl and A. Ratcliffe, Effects of long term growth on tissue engineered cartilage, *Trans. Orthop. Res. Soc.* **28** (2003), 309.
[3] T. Ahsan, L.M. Lottman, F. Harwood, D. Amiel and R.L. Sah, Integrative cartilage repair: inhibition by beta-aminopropionitrile, *J. Orthop. Res.* **17**(6) (1999), 850–7.
[4] T. Ahsan and R.L. Sah, Biomechanics of integrative cartilage repair, *Osteoarthritis Cartilage* **7**(1) (1999), 29–40.
[5] P. Angele, R. Kujat, M. Nerlich, J. Yoo, V. Goldberg and B. Johnstone, Engineering of osteochondral tissue with bone marrow mesenchymal progenitor cells in a derivatized hyaluronan-gelatin composite sponge, *Tissue Eng.* **5**(6) (1999), 545–54.
[6] G.A. Ateshian, M.A. Soltz, R.L. Mauck, I.M. Basalo, C.T. Hung and W.M. Lai, The role of osmotic pressure and tension–compression nonlinearity in the frictional response of articular cartilage, *Transport in Porous Media* **50** (2003), 5–33.
[7] P.D. Benya and J.D. Shaffer, Dedifferentiated chondrocytes reexpress the differentiated collagen phenotype when cultured in agarose gels, *Cell* **30**(1) (1982), 215–24.

[8] M. Brittberg, A. Nilsson, A. Lindahl, C. Ohlsson and L. Peterson, Rabbit articular cartilage defects treated with autologous cultured chondrocytes, *Clin. Orthop.* (326) (1996), 270–83.
[9] M.D. Buschmann, Y.A. Gluzband, A.J. Grodzinsky and E.B. Hunziker, Mechanical compression modulates matrix biosynthesis in chondrocyte/agarose culture, *J. Cell Sci.* **108** (Pt 4) (1995), 1497–508.
[10] M.D. Buschmann, Y.A. Gluzband, A.J. Grodzinsky, J.H. Kimura and E.B. Hunziker, Chondrocytes in agarose culture synthesize a mechanically functional extracellular matrix, *J. Orthop. Res.* **10**(6) (1992), 745–58.
[11] M.D. Buschmann and A.J. Grodzinsky, A molecular model of proteoglycan-associated electrostatic forces in cartilage mechanics, *J. Biomech. Eng.* **117**(2) (1995), 179–92.
[12] M.D. Buschmann, Y.J. Kim, M. Wong, E. Frank, E.B. Hunziker and A.J. Grodzinsky, Stimulation of aggrecan synthesis in cartilage explants by cyclic loading is localized to regions of high interstitial fluid flow, *Arch. Biochem. Biophys.* **366**(1) (1999), 1–7.
[13] A.I. Caplan, M. Elyaderani, Y. Mochizuki, S. Wakitani and V.M. Goldberg, Principles of cartilage repair and regeneration, *Clin. Orthop.* (342) (1997), 254–69.
[14] S.C. Chang, J.A. Rowley, G. Tobias, N.G. Genes, A.K. Roy, D.J. Mooney, C.A. Vacanti and L.J. Bonassar, Injection molding of chondrocyte/alginate constructs in the shape of facial implants, *J. Biomed. Mater. Res.* **55**(4) (2001), 503–11.
[15] D.T. Felson and Y. Zhang, An update on the epidemiology of knee and hip osteoarthritis with a view to prevention, *Arthritis Rheum.* **41**(8) (1998), 1343–55.
[16] L.E. Freed, R. Langer, I. Martin, N.R. Pellis and G. Vunjak-Novakovic, Tissue engineering of cartilage in space, *Proc. Natl. Acad. Sci. USA* **94**(25) (1997), 13885–90.
[17] L.E. Freed, N. Pellis, N. Searby, J. de Luis, C. Preda, J. Bordonaro and G. Vunjak-Novakovic, Microgravity cultivation of cells and tissues, *Gravit. Space Biol. Bull.* **12**(2) (1999), 57–66.
[18] F. Guilak, R.L. Sah and L.A. Setton, Physical regulation of cartilage metabolism, in: *Basic Orthopaedic Biomechanics*, W.C. Hayes, ed., Lippincott-Raven, Philadelphia, 1997, pp. 179–207.
[19] S.M. Haddock, J.C. Debes, E.A. Nauman, K.E. Fong, Y.P. Arramon and T.M. Keaveny, Structure–function relationships for coralline hydroxyapatite bone substitute, *J. Biomed. Mater. Res.* **47**(1) (1999), 71–8.
[20] L. Hangody, G. Kish, Z. Karpati, I. Szerb and I. Udvarhelyi, Arthroscopic autogenous osteochondral mosaicplasty for the treatment of femoral condylar articular defects. A preliminary report, *Knee Surg. Sports Traumatol. Arthrosc.* **5**(4) (1997), 262–7.
[21] M.C. Harper, Viscous isoamyl 2-cyanoacrylate as an osseous adhesive in the repair of osteochondral osteotomies in rabbits, *J. Orthop. Res.* **6**(2) (1988), 287–92.
[22] C.D. Hoemann, J. Sun, V. Chrzanowski and M.D. Buschmann, A multivalent assay to detect glycosaminoglycan, protein, collagen, RNA, and DNA content in milligram samples of cartilage of hydrogel-based repair cartilage, *Anal. Biochem.* **300**(1) (2002), 1–10.
[23] C.Y. Huang, V.C. Mow and G.A. Ateshian, The role of flow-independent viscoelasticity in the biphasic tensile and compressive responses of articular cartilage, *J. Biomech. Eng.* **123**(5) (2001), 410–7.
[24] C.T. Hung, E.G. Lima, R.L. Mauck, M.A. LeRoux, E. Takai, H.H. Lu, R.G. Stark, X.E. Guo and G.A. Ateshian, Anatomically shaped osteochondral constructs for articular cartilage repair, *J. Biomechanics* **36** (2003), 1853–64.
[25] Y.J. Kim, R.L. Sah, A.J. Grodzinsky, A.H. Plaas and J.D. Sandy, Mechanical regulation of cartilage biosynthetic behavior: physical stimuli, *Arch. Biochem. Biophys.* **311**(1) (1994), 1–12.
[26] D.A. Lee and D.L. Bader, Compressive strains at physiological frequencies influence the metabolism of chondrocytes seeded in agarose, *J. Orthop. Res.* **15**(2) (1997), 181–8.
[27] D.A. Lee, T. Noguchi, S.P. Frean, P. Lees and D.L. Bader, The influence of mechanical loading on isolated chondrocytes seeded in agarose constructs, *Biorheology* **37**(1–2) (2000), 149–61.
[28] E.G. Lima, R.L. Mauck, S. Gasinu, G.A. Ateshian and C.T. Hung, Functional tissue engineering of free swelling and dynamically loaded osteochondral constructs, *Trans. Orthop. Res. Soc.* **29** (2004), 13.
[29] T. Livingston, P. Ducheyne and J. Garino, In vivo evaluation of a bioactive scaffold for bone tissue engineering, *J. Biomed. Mater. Res.* **62**(1) (2002), 1–13.
[30] H.J. Mankin, The response of articular cartilage to mechanical injury, *J. Bone Joint Surg.* **64-A**(460-66) (1982).
[31] R.L. Mauck, S.B. Nicoll, S.L. Seyhan, G.A. Ateshian and C.T. Hung, Synergistic action of growth factors and dynamic loading for articular cartilage tissue engineering, *Tiss. Eng.* **9**(4) (2003), 597–611.
[32] R.L. Mauck, S.L. Seyhan, G.A. Ateshian and C.T. Hung, Influence of seeding density and dynamic deformational loading on the developing structure/function relationships of chondrocyte-seeded agarose hydrogels, *Ann. Biomed. Eng.* **30**(8) (2002), 1046–56.
[33] R.L. Mauck, M.A. Soltz, C.C. Wang, D.D. Wong, P.H. Chao, W.B. Valhmu, C.T. Hung and G.A. Ateshian, Functional tissue engineering of articular cartilage through dynamic loading of chondrocyte-seeded agarose gels, *J. Biomech. Eng.* **122**(3) (2000), 252–60.
[34] R.L. Mauck, C.C.-B. Wang, Q. Cheng, N. Gabriel, H.H. Lu, F.H. Chen, G.A. Ateshian and C.T. Hung, Optimization of parameters of for articular cartilage tissue engineering with deformational loading, *Trans. Orthop. Res. Soc.* **28** (2003).

[35] R.L. Mauck, C.C.-B. Wang, E.S. Oswald, F.H. Chen, G.A. Ateshian and C.T. Hung, The role of cell seeding density and nutrient supply for articular cartilage tissue engineering with deformational loading, *Osteoarthritis and Cartilage* **11** (2003), 879–890.
[36] V.C. Mow, N.M. Bachrach, L.A. Setton and F. Guilak, Stress, strain, pressure, and flow fields in articular cartilage and chondrocytes, in: *Cell Mechanics and Cellular Engineering*, R.M. Hochmuth, ed., Springer-Verlag, New York, 1994, p. 345–79.
[37] V.C. Mow and X.E. Guo, Mechano-electrochemical properties of articular cartilage: their inhomogeneities and anisotropies, *Annu. Rev. Biomed. Eng.* **4** (2002), 175–209.
[38] V.C. Mow, S.C. Kuei, W.M. Lai and C.G. Armstrong, Biphasic creep and stress relaxation of articular cartilage in compression? Theory and experiments, *J. Biomech. Eng.* **102**(1) (1980), 73–84.
[39] V.C. Mow and C.C. Wang, Some bioengineering considerations for tissue engineering of articular cartilage, *Clin. Orthop.* (367 Suppl.) (1999), S204–23.
[40] K.W. Ng, C.C.-B. Wang, X.E. Guo, G.A. Ateshian and C.T. Hung, Characterization of inhomogeneous bi-layered chondrocyte-seeded agarose constructs of differing agarose concentrations, *Trans. Orthop. Res. Soc.* **28** (2003), 960.
[41] S.W. O'Driscoll, F.W. Keeley and R.B. Salter, The chondrogenic potential of free autogenous periosteal grafts for biological resurfacing of major full-thickness defects in joint surfaces under the influence of continuous passive motion. An experimental investigation in the rabbit, *J. Bone Joint Surg. Am.* **68**(7) (1986), 1017–35.
[42] B. Obradovic, I. Martin, R.F. Padera, S. Treppo, L.E. Freed and G. Vunjak-Novakovic, Integration of engineered cartilage, *J. Orthop. Res.* **19**(6) (2001), 1089–97.
[43] K.T. Paige, L.G. Cima, M.J. Yaremchuk, J.P. Vacanti and C.A. Vacanti, Injectable cartilage, *Plast. Reconstr. Surg.* **96**(6) (1995), 1390–8; discussion 1399–400.
[44] S. Park, C.T. Hung and G.A. Ateshian, Mechanical response of bovine articular cartilage under dynamic unconfined compression loading at physiological stress levels, *Osteoarthritis Cartilage* **12**(1) (2003), 65–73.
[45] D. Pazzano, K.A. Mercier, J.M. Moran, S.S. Fong, D.D. DiBiasio, J.X. Rulfs, S.S. Kohles and L.J. Bonassar, Comparison of chondrogensis in static and perfused bioreactor culture, *Biotechnol. Prog.* **16**(5) (2000), 893–6.
[46] D. Schaefer, I. Martin, G. Jundt, J. Seidel, M. Heberer, A. Grodzinsky, I. Bergin, G. Vunjak-Novakovic and L.E. Freed, Tissue-engineered composites for the repair of large osteochondral defects, *Arthritis Rheum.* **46**(9) (2002), 2524–34.
[47] D. Schaefer, I. Martin, P. Shastri, R.F. Padera, R. Langer, L.E. Freed and G. Vunjak-Novakovic, In vitro generation of osteochondral composites, *Biomaterials* **21**(24) (2000), 2599–606.
[48] J.K. Sherwood, S.K. Riley, R. Palazzolo, S.C. Brown, D.C. Monkhouse, M. Coates, L.G. Griffith, L.K. Landeen and A. Ratcliffe, A three-dimensional osteochondral composite scaffold for articular cartilage repair, *Biomaterials* **23**(24) (2002), 4739–51.
[49] M.A. Soltz and G.A. Ateshian, A Conewise Linear Elasticity mixture model for the analysis of tension–compression nonlinearity in articular cartilage, *J. Biomech. Eng.* **122**(6) (2000), 576–86.
[50] E. Takai, E.G. Lima, H.H. Lu, G.A. Ateshian, X.E. Guo and C.T. Hung, Devitalized bone as a mineralized substrate for osteochondral tissue engineered hydrogel constructs, *Trans. Orthop. Res. Soc.* **28** (2003), 307.
[51] G. Vunjak-Novakovic, I. Martin, B. Obradovic, S. Treppo, A.J. Grodzinsky, R. Langer and L.E. Freed, Bioreactor cultivation conditions modulate the composition and mechanical properties of tissue-engineered cartilage, *J. Orthop. Res.* **17**(1) (1999), 130–8.
[52] G. Vunjak-Novakovic, B. Obradovic, I. Martin and L.E. Freed, Bioreactor studies of native and tissue engineered cartilage, *Biorheology* **39**(1–2) (2002), 259–68.
[53] C.C. Wang, J.M. Deng, G.A. Ateshian and C.T. Hung, An automated approach for direct measurement of two-dimensional strain distributions within articular cartilage under unconfined compression, *J. Biomech. Eng.* **124**(5) (2002), 557–67.
[54] C.C. Wang, X.E. Guo, D. Sun, V.C. Mow, G.A. Ateshian and C.T. Hung, The functional environment of chondrocytes within cartilage subjected to compressive loading: a theoretical and experimental approach, *Biorheology* **39**(1–2) (2002), 11–25.
[55] C.C. Wang, C.T. Hung and V.C. Mow, An analysis of the effects of depth-dependent aggregate modulus on articular cartilage stress-relaxation behavior in compression, *J. Biomech.* **34**(1) (2001), 75–84.
[56] C.C.-B. Wang, T.N. Kelly, R.L. Mauck, G.A. Ateshian and C.T. Hung, Temporal and spatial development of construct stiffness in chondrocyte-seeded agarose disks cultured in free-swelling and dynamical-loading configurations, *ASME-BED* (Summer Meeting) (2003), 279–280.
[57] C.C.-B. Wang, M.A. Soltz, R.L. Mauck, W.B. Valhmu, G.A. Ateshian and C.T. Hung, Comparison of the equilibrium axial strain distribution in articular cartilage explants and cell-seeded alginate disks under unconfined compression, *Trans. Orthop. Res. Soc.* **25** (2000), 131.
[58] C.C.B. Wang, N.O. Chahine, C.T. Hung and G.A. Ateshian, Optical determination of anisotropic properties of bovine articular cartilage in compression, *J. Biomech.* **36**(3) (2003), 339–53.

[59] Y. Weng, Y. Cao, C.A. Silva, M.P. Vacanti and C.A. Vacanti, Tissue-engineered composites of bone and cartilage for mandible condylar reconstruction, *J. Oral Maxillofac. Surg.* **59**(2) (2001), 185–190.
[60] J.Z. Wu, W. Herzog and E.M. Hasler, Inadequate placement of osteochondral plugs may induce abnormal stress–strain distributions in articular cartilage – finite element simulations, *Med. Eng. Phys.* **24**(2) (2002), 85–97.
[61] B.J. Zuger, B. Ott, P. Mainil-Varlet, T. Schaffner, J.F. Clemence, H.P. Weber and M. Frenz, Laser solder welding of articular cartilage: tensile strength and chondrocyte viability, *Lasers Surg. Med.* **28**(5) (2001), 427–34.